# Variable Intensity of Lagrangian Chaos in the Nonlinear Dynamo Problem

E. Zienicke, H. Politano, and A. Pouquet

*CNRS, UMR 6529, Observatoire de la Côte d'Azur, B.P. 4229 06304 Nice Cedex 4, France*

(Received 30 April 1998; revised manuscript received 11 September 1998)

The link between the level of chaos of the velocity and the saturation of the dynamo in *ABC* flows is examined numerically with the full MHD equations at magnetic Reynolds numbers up to 240 and for scale separations up to four. In the latter case, a chaotic dynamo at small scale and a large-scale magnetic field develop together. Spatial modifications of the chaotic features of the resulting velocity measured by *pdf* of finite-time Lyapunov exponents occur in all cases because of both hydrodynamic and MHD instabilities. Saturation occurs as well with a weaker contrast in magnetic structures. [S0031-9007(98)07723-0]

PACS numbers: 47.65.+a, 05.45.+b, 47.27.Gs, 91.25.Cw

Magnetic fields are ubiquitous in the Universe, often embedded in turbulent flows. For example, in the solar atmosphere as well as in the interstellar medium, there is ample evidence for turbulent motions and for both small-scale and large-scale magnetic fields, the former roughly in equipartition with the motions of the eddies. In the solar case, observations also indicate the presence of strong filamentary magnetic structures with a large contrast with the background field. Such fields are either primordial or due to a generation mechanism from a small magnetic seed through the dynamo effect. The linear phase or kinematic dynamo—neglecting the reaction of the magnetic field on the turbulent motions that give rise to it—is well documented; the magnetic field grows both at large scale, because of small-scale kinetic helicity (the so-called $\alpha$ effect), and at small scale because of the chaotic properties of the underlying flow (see, e.g., [1,2] for reviews). However, the nonlinear regime is less understood. The back reaction of the magnetic field on the velocity can be modelized, e.g., with the help of closures of turbulence [3,4]; they indicate that saturation may occur through helical Alfvén waves provided a large-scale magnetic field exists, a field which develops through an inverse cascade of magnetic helicity $H^M = \langle \mathbf{a} \cdot \mathbf{b} \rangle$ with $\mathbf{b} = \nabla \times \mathbf{a}$ the magnetic induction; this cascade takes place independently of the velocity structures since the invariance of $H^M$ stems from the induction equation alone. Models [3,5] and computations in the incompressible [6,7] and compressible cases—both subsonic [8] and supersonic [9]—indicate linear growth of magnetic helicity, including in the nonlinear dynamo regime.

A mechanism has also been suggested whereby saturation of the dynamo occurs because of the intermittent filamentary nature of the magnetic field [10], a filamentation observed both in astrophysical flows as mentioned earlier as well as in several numerical simulations [11–13]. The intermittency of the growing magnetic field could be due to the fact that only in localized regions of space can a velocity field stretch, twist, and fold the magnetic field lines, e.g., in the vicinity of stagnation points (of measure zero), as obtained in kinematic dynamos in *ABC* flows [13]. These strong tubes can reconnect, thereby locally reducing magnetic energy without affecting globally the turbulent velocity field. Indeed, in the saturation regime of the *ABC* dynamo, filaments disappear and weaker sheets are prevalent [11,14], at least at modest Reynolds numbers.

On the other hand, the interesting conjecture that the underlying Lagrangian chaos may be suppressed by a strong magnetic field as a mechanism of nonlinear saturation [15] is backed up by a series of numerical calculations up to magnetic Reynolds numbers of $R^M = 100$ and with $P^M = 4$ where $P^M = \nu/\eta$ is the magnetic Prandtl number, $\nu$ and $\eta$ being the viscosity and the magnetic diffusivity. This is done in the framework of a model within which several key assumptions are made: (i) The advection term responsible in an incompressible fluid for the turbulence is suppressed, allowing for a simple decomposition of the kinematic/dynamic phases of the dynamo; (ii) the influence of the Lorentz force is assumed to let the flow retain a two-dimensional character; (iii) the magnetic field can develop only at scales smaller than or equal to that of the forcing flow. With these assumptions, a clear diminution of chaos—as diagnosed by a two-dimensional map of finite-time Lyapunov exponents—is obtained.

The purpose of this paper is to tackle the same problem dropping all three assumptions. Computations are presented here up to $R^M = 240$ (see [16]) using a pseudospectral Fourier method with periodic boundary conditions and a forcing corresponding to the standard $ABC_{k_0}$ flow with $A = B = C$ at a characteristic wave number of $k_0 = 1$, 2, or 4 (with $k_{\min} = 1$ corresponding to the largest scale $L_0 = 2\pi$ in the box). The Reynolds numbers remain low and thus this work is not concerned with the fast dynamo proper, which deals with the limit $R^M \to \infty$. Nevertheless, the fact that the velocity field is allowed to destabilize to a more turbulent configuration—as measured, for example, by its departure from a superposition of pure Beltrami waves [17]—means that the kinetic Reynolds number $R^V$ in the computations here is not

 0031-9007/98/81(21)/4640(4)$15.00 

limited to low values (the standard $ABC_1$ flow destabilizes [17] for $R^V \approx 13$).

A dimensionalizing velocity and length scales with, respectively, $A$ and $\ell_0/2\pi = 1/k_0$, the MHD equations write:

$$(\partial_t + \mathbf{v}\cdot\nabla)\mathbf{v} = -\nabla P + \mathbf{j}\times\mathbf{b} + (\nabla^2\mathbf{v} + \mathbf{U}_{111}^{k_0})/R^V, \quad (1)$$

$$(\partial_t + \mathbf{v}\cdot\nabla)\mathbf{b} = \mathbf{b}\cdot\nabla\mathbf{v} + \nabla^2\mathbf{b}/R^M, \quad (2)$$

where $\mathbf{v}$ is the velocity, $P$ the pressure, $\mathbf{j} = \nabla\times\mathbf{b}$ the current density, and $\nabla\cdot\mathbf{v} = 0$, $\nabla\cdot\mathbf{b} = 0$. In the forcing term, $\mathbf{U}_{ABC}^{k_0} = (A\sin k_0 z + C\cos k_0 y, B\sin k_0 x + A\cos k_0 z, C\sin k_0 y + B\cos k_0 x)$ is a Beltrami flow ($\nabla\times\mathbf{U}_{ABC}^{k_0} = k_0\mathbf{U}_{ABC}^{k_0}$) and consists of three helical waves whose characteristic scale $\ell_0$ is used to define all Reynolds numbers quoted here [16].

We integrate numerically Eqs. (1) and (2), and we choose for convenience $A = k_0$. The code is parallelized with HTMF for the Cray-T3E and uses a second-order Adams-Bashforth/Cranck-Nicholson temporal scheme. With 64 processors, one time step needs 0.7 s for $128^3$ grid points.

The streamlines of the $ABC_1$ flow are known to be chaotic [18], and $ABC$ flows are prototypes for the study of dynamos both in the kinematic [13,19] and in the nonlinear regimes [11]. In particular, two mechanisms for growth were identified in [11], provided there be sufficient scale separation between $\ell_0$ and $L_0$. That $ABC$ flows may indeed lead to a fast dynamo is shown strikingly in the context of temporally varying flows with $C = 0$, in which case the independence of modes in the third direction allows for two-dimensional computations at high $R^M$ [20].

The numerical setup is similar to that described in [11]. In a first nonmagnetic phase, the velocity field is left to settle to a statistically steady state, a seed magnetic field of total energy $10^{-9}$ is then introduced and distributed evenly between all Fourier modes in the first six shells. Finite-time local first Lyapunov exponents for the underlying resulting velocity fields $\lambda_{k_0}(\mathbf{x})$, together with their mean $\bar{\lambda}_{k_0}$ and their maxima $\lambda_{k_0}^M$, are computed as the MHD integration proceeds, using $128^2$ fluid particles started at a chosen time in the plane $x = \pi/2$.

The trajectories inside the cube are given by the three dimensional system of ordinary differential equations $\dot{\mathbf{x}} = \mathbf{v}(\mathbf{x}, t)$. At each time step, the actual velocity field is trigonometrically interpolated (up to a number of shells $k_M$) at the momentary position of each fluid particle to carry out the integration of the trajectories. The finite-time approximation of the highest Lyapunov exponent is computed for each trajectory in the usual way [21]. As the interpolation of the velocity field for each time step needs communication between processors and $\propto k_M^3$ operations, there is a ninefold increase in computation time for $128^3$ grid points, as compared to the integration of the MHD equations alone, with $k_M = 15$. All initial conditions, in the $x = \pi/2$ plane, are followed for a time interval $\Delta T$ between 80 and 320 kinematic turnover times $\tau_{NL} = (Ak_0)^{-1}$ of the $ABC_{k_0}$ flow. Comparisons between the different phases for a given run are performed on the same time interval, with as a limitation the length of the growing phase of the dynamo. Starting in the plane $x = 4$ instead of $x = \pi/2$ leads to the same results for $\bar{\lambda}_{k_0}$ within less than 5%, as checked on the $ABC_1$ case.

We first evaluate the amount of chaos in a dynamo at a Reynolds number for which the $ABC_1$ flow is stable. For $R^V = R^M = 12$, the dynamo saturates below equipartition [11], with the ratio of magnetic to kinetic energy $\chi = E^M/E^V \approx 0.03$. In Fig. 1 are shown the histograms of the finite-time Lyapunov exponents for the growth phase (dashed line) and the final saturation phase (solid line) computed for $\Delta T = 320$. The means are, respectively, 1.3 and 3.5 (in units of $\bar{\lambda}_1 = 0.015$ for $ABC_1$), and the maxima are, respectively, 0.14 and 0.27 (in units of $\lambda_1^M = 0.7$). Thus, the modifications to the $ABC_1$ flow—here, due only to the magnetic instability—*enhance* chaos in the mean in the saturated dynamo phase by a factor of almost 3 on average, with a strong tail of local values up to $11.3\bar{\lambda}_1$, although local chaos as measured by $\lambda_1^M$ seems to be substantially stronger in the $ABC_1$ flow itself, because at one isolated point, the grid chosen initially coincides exactly with an unstable manifold.

Keeping $k_0 = 1$, we performed a run with $R^V = 60$ (for which the velocity is unstable) and $R^M = 240$. The saturated ratio of energies is now increased to $\chi \approx 0.12$. Lyapunov exponents are given in the form of gray scale images in the plane $x = \pi/2$ in Fig. 2, with $\Delta T = 80$: $ABC_1$ flow (left), statistically steady resulting velocity and magnetic growth phase—which lasts $\approx\Delta T$—(center) and saturation phase (right). Mean exponents are, respectively, 2.8 and 1.8 for the latter two, in units of the mean for the destabilized velocity, i.e., 0.040.

The $ABC_1$ flow evolves—albeit slowly—towards a more turbulent configuration with all shells excited [17] and, as shown here, towards a more chaotic state as well.

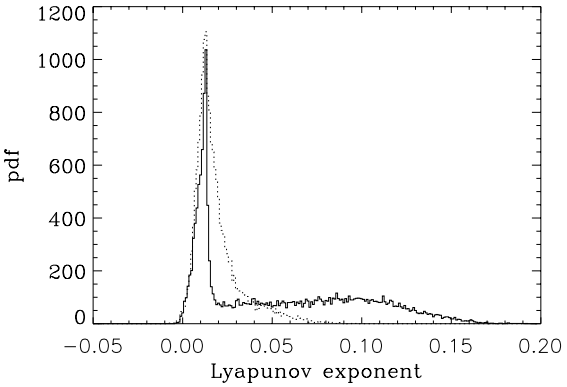


FIG. 1. Finite-time Lyapunov exponents, $R^V = R^M = 12$, $k_0 = 1$; growth (dashed line) and nonlinear (solid line) phases.

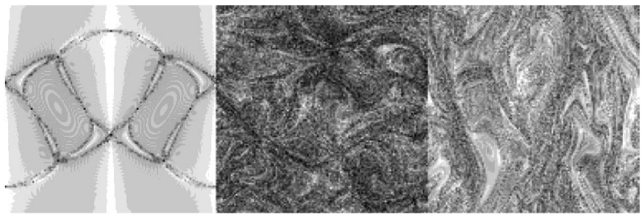

FIG. 2. Images ranging from 0 (white) to 0.25 (black) of finite-time Lyapunov exponents, $R^V = 60$, $R^M = 240$; $ABC_1$ flow (left), growth phase (center), and saturation (right).

Once the magnetic field has grown sufficiently, it is able to reduce to some extent the amount of chaos, by less than a factor of 2 on average; thus, the saturation does occur with a decrease of chaos compared to the growth phase, but with, however, a substantially more complex velocity field than the starting $ABC_1$ velocity itself. This can be understood by realizing that the motions have to work against the rigidity of magnetic field lines. Indeed, both the **v** and **b** fields are less turbulent as well, as indicated by a larger gap in the modal energy between the excited mode and its nearest neighbors (not shown). The fact that the magnetic field organizes in strong localized structures centered on stagnation points of the velocity allows the turbulent field to develop everywhere else [11], thus reaching an as yet uneven balance between kinetic and magnetic energy.

Letting the unstable perturbations develop at scales larger than $\ell_0$ plays a crucial role in determining the growth rate of the magnetic field [11] and the structures that develop [11,22]. A run with $k_0 = 2$ and $R^V = 60$, $R^M = 240$ indicates that for the $ABC_2$ flow $\bar{\lambda}_2 = 0.027$ and $\lambda_2^M = 0.7$ (computed for $\Delta T = 160$), whereas in the growth (respectively, saturation) phase the mean is $3.5\bar{\lambda}_2$ and the maximum $0.28\lambda_2^M$ (respectively, a mean of $1.7\bar{\lambda}_2$ and a maximum of $0.14\lambda_2^M$). Contrasted with the growth phase, the mean Lyapunov exponents of the resulting velocity are much larger simply because the flow has many more excited modes, but saturation does result again in a diminution of chaos by a factor of 2 on average. This more quiescent state of the velocity in the final stage is detectable by inspection of the temporal evolution of modal energies (see also [11]): at saturation and rather abruptly (not shown), the kinetic energy density spectrum $E_k^V$ in shells 1 and 3 drops, resulting in a spectral gap with $E_{k=2}^V \approx 10E_{k=3}^V$. For that same run, we show in Fig. 3 the ratio of the maximum to the rms values of the magnetic field (solid line) and the velocity (dashed line): the strong intermittency of the magnetic field is drastically reduced at saturation, with weaker dynamical contrast for magnetic structures, from filaments to sheets, as already noted in [7]; a comparable drop obtains for all runs reported here. For all runs, velocities systematically display a substantially weaker contrast.

We now measure for the $ABC_2$ flow the averaged nonlinear magnetic energy transfer $T_1 = \langle \mathbf{v} \cdot (\mathbf{b} \times \mathbf{j}) \rangle$, and

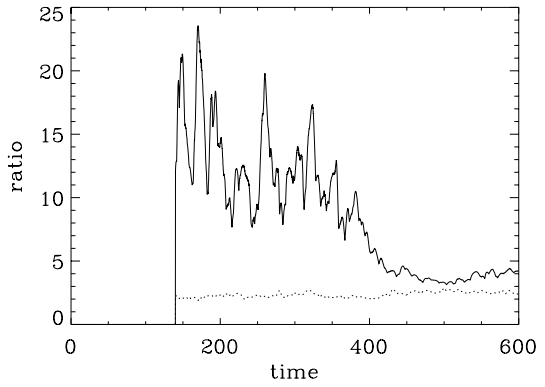


FIG. 3. Ratio of maximum to rms magnetic field (solid line) and velocity (dashed line) for the $ABC_2$ dynamo at $R^M = 240$.

normalized as $T_2 = T_1/\sqrt{\langle \mathbf{j}^2 \rangle \langle \mathbf{b}^2 \rangle}$ and $T_3 = T_2/\sqrt{\langle \mathbf{v}^2 \rangle}$ ($T_1$ is not optimal in the growth phase where **b** starts at very low values). Temporal variations of $T_i$ are given in Fig. 4, with $T_1$ (respectively, $T_2$ and $T_3$) in solid line (respectively, dashed and dotted lines). An overshoot of transfer (seen on $T_1$) marks the end of the growth phase. For $T_{2,3}$, one finds a nearly constant value for both the growth and saturated phases, smaller in the latter phase. The drop from the growth to the saturated phase is smaller for $T_3$, indicating that saturation does not arise mainly from a geometric reconfiguration of the $(\mathbf{v}, \mathbf{b}, \mathbf{j})$ fields.

The symmetry breaking induced by letting $L_0 \neq \ell_0$ results in an overall stronger chaos. However, the $\alpha$ effect itself, in its analytical demonstration, requires a measurable scale separation, costly from a numerical point of view, and a nongrowing small scale magnetic field as well. Hence, including and analyzing this mechanism is limited up to now to moderate Reynolds numbers [6,7,11] (unless the large scales are blocked as in [23]).

At $R^V = R^M = 12$—similarly to the magnetic case where the Reynolds number above which instability occurs is substantially lowered when modes corresponding to scales larger than $\ell_0$ are free to grow—here again for $k_0 = 4$, the $ABC$ flow is hydrodynamically unstable,

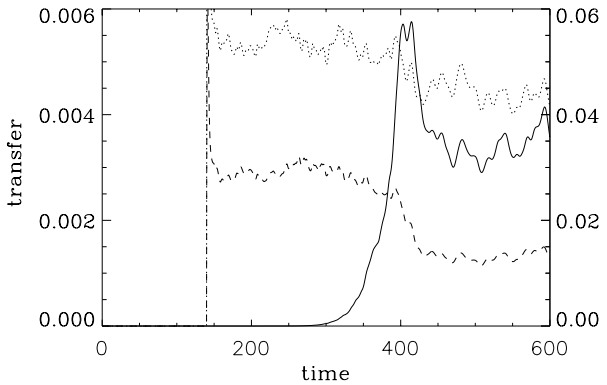


FIG. 4. Magnetic energy transfer with different normalizations for the $ABC_2$ flow: $T_1$ (solid line, left scale); $T_2$ with dash and $T_3$ with dot (for both, right scale).

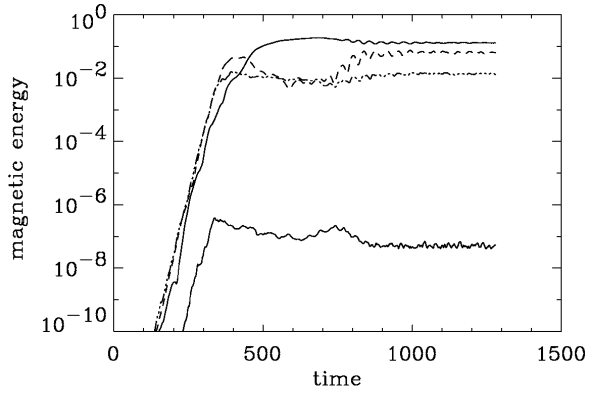


FIG. 5. Evolution of magnetic shells, $R^V = R^M = 12$, $k_0 = 4$; $k = 1$ (respectively, 2 and 4) in solid line (respectively, dashed and dash-dotted lines).

whereas it is stable for $k_0 = 1$. We show in Fig. 5 the evolution of several magnetic Fourier shells (the lower line represents the last shell with modal energy $\approx 10^{-6}$ that of the largest scale, indicative of adequate numerical resolution). Three phases can be identified: (i) A growth phase up to $t \approx 320$; (ii) a first saturation phase up to $t \approx 700$ where $E^M_{k=1} > E^M_{k=4} > E^M_{k=2}$; and finally (iii) a second saturation phase where the modal energy for $k = 2$ has now surpassed that of the forcing mode. Phases (ii) and (iii) can also be distinguished when examining (not shown) the temporal evolution of both the relative kinetic and magnetic helicity; the former finally oscillates around 0.77, whereas the latter settles at a value of $-0.52$, thus at rather close absolute values indicative that helicity may be at play for this dynamo [3]. In this case again, chaos is stronger on average in the growth phase of the dynamo with a mean Lyapunov exponent of $3.5\bar{\lambda}_4$ (and a maximum of $0.27\lambda^M_4$ where $\bar{\lambda}_4 = 0.031$ and $\lambda^M_4 = 0.7$ for $\Delta T = 160$), and with a subsequent diminution to $2.0\bar{\lambda}_4$ for the mean and $0.16\lambda^M_4$ for the maximum in the saturated phase.

The results presented in this paper indicate that, when letting the velocity field destabilize, a chaos stronger on average (but weaker locally) than for the rather quiescent driving develops in the growth phase of the dynamo. Subsequently, this chaos, as conjectured in [15], is diminished to a measurable extent in the final (saturation) phase. However, these results may be Reynolds dependent. Computations achieving both a reasonably high Reynolds number together with an acceptable scale separation require important CPU and storage resources, with possible resort (for the former) to an hyperviscosity algorithm as in [24]. Such computations are much in demand to further analyze the issues related to the saturation mechanisms of dynamos important in the astrophysical context and as yet unsolved.

Computations were done on T3E/IDRIS (Orsay). We are pleased to acknowledge financial support from CNRS-1202-MFGA and EEC-ERBCHRXCT930410.

[1] H. K. Moffatt, *Magnetic Field Generation in Electrically Conducting Fluids* (Cambridge University Press, Cambridge, England, 1978).
[2] S. Childress and A. Gilbert, *Stretch, Twist, Fold: The Fast Dynamo* (Springer-Verlag, Berlin, 1995).
[3] A. Pouquet, U. Frisch, and J. Léorat, J. Fluid Mech. **77**, 321 (1976).
[4] A. Gruzinov and P. Diamond, Phys. Rev. Lett. **72**, 1651 (1994); A. Bhattacharjee and Y. Yuan, Astrophys. J. **449**, 739B (1995).
[5] U. Frisch *et al.*, J. Fluid Mech. **68**, 769 (1975).
[6] A. Pouquet and G. S. Patterson, J. Fluid Mech. **85**, 305 (1978).
[7] M. Meneguzzi, U. Frisch, and A. Pouquet, Phys. Rev. Lett. **47**, 1060 (1981).
[8] R. Horiuchi and T. Sato, Phys. Fluids **31**, 1142 (1988).
[9] D. Balsara and A. Pouquet, Phys. Plasmas (to be published).
[10] E. Blackman, Phys. Rev. Lett. **77**, 2694 (1996).
[11] B. Galanti, thesis, Université de Nice, 1991; B. Galanti, P. L. Sulem, and A. Pouquet, Geophys. Astrophys. Fluid Dyn. **66**, 183 (1992).
[12] A. Brandenburg *et al.*, J. Fluid Mech. **306**, 325 (1996).
[13] D. Galloway and U. Frisch, Geophys. Astrophys. Fluid Dyn. **36**, 53 (1986).
[14] D. J Galloway and N. R. O'Brian, in *Theory of Solar and Planetary Dynamos*, edited by M. R. E. Proctor, P. C. Matthews, and A. M. Rucklidge (Cambridge University Press, Cambridge, England, 1993), p. 105.
[15] F. Cattaneo, D. Hughes, and E. Kim, Phys. Rev. Lett. **76**, 2057 (1996).
[16] $R^V \equiv \ell_0 A/2\pi\nu$ [respectively, $R^M = \ell_0 A/2\pi\eta$] is the kinetic (respectively, magnetic) Reynolds number evaluated with the amplitude of the force. One could also define Reynolds numbers based on the rms velocity once the *ABC* flow (unstable [17] above $R^V \approx 13$ for $k_0 = 1$, and for $k_0 \neq 1$ as shown here) has settled. The latter are typically lower by a factor of 4.
[17] D. Galloway and U. Frisch, J. Fluid Mech. **180**, 557 (1987); O. Podvigina and A. Pouquet, Physica (Amsterdam) **75D**, 475 (1994).
[18] T. Dombre *et al.*, J. Fluid Mech. **167**, 353 (1986).
[19] V. Arnol'd and E. Korkina, Vestn. Mosk. Univ. 1, Mat. Mekh. **38**, 43 (1983).
[20] D. Galloway and M. Proctor, Nature (London) **356**, 691 (1993); Y. Ponty, A. Pouquet, and P. L. Sulem, Geophys. Astrophys. Fluid Dyn. **79**, 239 (1995).
[21] E. Ott, *Chaos in Dynamical Systems* (Cambridge University Press, Cambridge, England, 1993).
[22] With $\langle b^2 \rangle \propto e^{\gamma_i t}$, we find $\gamma_1 = 0.07, \gamma_2 = 0.07$, and $\gamma_4 = 0.09$ referring to three runs with $k_{0;i} = 1$, 2, and 4, respectively. In that light, it would be interesting to analyze the possible changes in growth rates and cancellation exponents, and their variations with $R^M$, for *ABC* flows with identical chaotic properties but different magnetic helicity as performed for $k_0 = 1$ in D. Hughes, F. Cattaneo, and E. Kim, Phys. Lett. A **223**, 167 (1996).
[23] F. Cattaneo and D. Hughes, Phys. Rev. E **54**, R4532 (1996).
[24] S. Kida, S. Yanase, and J. Mizushima, Phys. Fluids A **3**, 457 (1991).